Additive Manufacturing: Metallurgy, Cut Analysis & Porosity

12 Advanced Optical Metrology

Additive Manufacturing:
Metallurgy, Cut Analysis & Porosity

EVIDENT
OLYMPUS

WILEY

The latest eBook from Advanced Optical Metrology. Download for free.
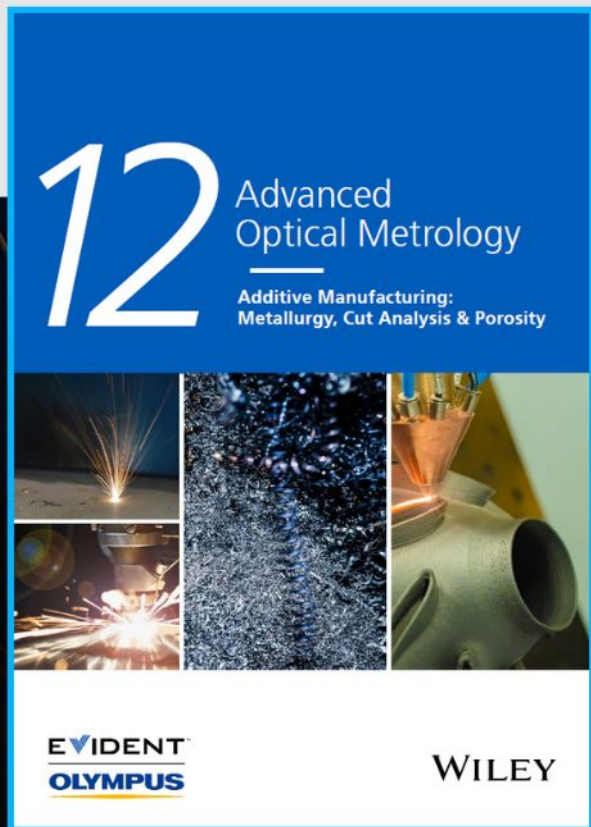
In industry, sector after sector is moving away from conventional production methods to additive manufacturing, a technology that has been recommended for substantial research investment.

Download the latest eBook to read about the applications, trends, opportunities, and challenges around this process, and how it has been adapted to different industrial sectors.

EVIDENT
OLYMPUS

WILEY

Rapidly Deformable Vitrimer Epoxy System with Supreme Stress-Relaxation Capabilities via Coordination of Solvate Ionic Liquids

Jae-Ho Shin, Mo-Beom Yi, Tae-Hyung Lee, and Hyun-Joong Kim*

Vitrimer epoxy, capable of stress-relaxation, has gathered attention for its ability to counter the brittleness and rigidity of thermosets. However, to date, only two strategies are proposed to address the high enthalpic barrier of a dynamic exchange reaction using high dosages of external catalysts or niche moieties as internal catalysts. Herein, solvate ionic liquids (SILs) are incorporated into commercial epoxy-based vinylogous urethane (VU) vitrimers. During curing, the SILs facilitate epoxy ring-opening and amine-addition reactions, significantly reducing gel times. Furthermore, after network formation, the SILs accelerate transamination reaction within the VU networks at a dosage of only 0.5–2 mol%. This can be attributed to their high miscibilities and Lewis acidic characters, which significantly reduce the activation energy of transamination (24 kJ mol^{-1}) in the SIL-incorporated vitrimer. Thus, a high-performing vitrimer epoxy is prepared, featuring a glassy modulus ($>10^9$ Pa) at room temperature and an extremely short stress-relaxation time ($\approx$19 s) at 160 °C. Moreover, a soft encapsulation approach is demonstrated using the vitrimer epoxy, proving the possibility of a simultaneous deformable (bent) encapsulation, reduced warpage of a flexible printed circuit board, and selective removal of encapsulants.

1. Introduction

Vitrimers, a term coined by Leibler et al. in 2011,[1] have proven to be an advanced class of polymeric materials capable of rearranging their cross-linked topology via associative dynamic exchange reactions while maintaining a constant number of networks in the system at service temperature. When a vitrimer is thermally triggered, it exhibits a characteristic transition from an elastic solid to a viscoelastic liquid in the Arrhenius manner.[2] On a microscopic level, dynamically exchangeable moieties rapidly reach thermodynamic equilibrium and operate degenerate reactions in percolated systems, allowing the network to flow.[3] During the topological rearrangement, vitrimers undergo stress-relaxation cycles while retaining their integrity. This advantage of vitrimers has drawn considerable attention from industries requiring novel polymeric materials to address the issue of stress.

Epoxy vitrimers are a multifunctional class of materials, affording high mechanical strength, excellent adhesion, and the (re)processibility and stress-relaxation abilities. Various dynamic chemistry routes, including transesterification,[4] transamination,[5] and imine metathesis,[6] have been investigated for epoxy vitrimers in recent years. However, attempts to enrich and expand their scope have resulted in many deviations from the existing epoxy formulations, which demand specific non-commercial resins and hardeners, with formulations differing from the conventional ones. This has limited the industrial application of vitrimer, and despite several attempts, there have been few reports on their multiple-processability or self-healing abilities to date. Therefore, the development of a more facile and robust design of epoxy-based vitrimers is necessary to expand their potential applications.

To function sufficiently, dynamic exchange reactions for epoxy-based vitrimers require an elevated temperature and an extended time scale. Many attempts have been made to adjust the time-temperature scale, such as the construction of niche polymer systems[7] or modification of the compositions of exchangeable moieties.[4f,6a,8] However, using catalysts with 1K resins is industrially more feasible than using unstandardized resins or undefined recipes. Conventionally, zinc acetate (Zn(OAc)$_2$) has been extensively used as a catalyst in epoxy vitrimer systems.[2,4a,b,5c] The Zn^{2+} ion interacts with carboxylates to form O-ligand/Zn(II) complexes, which serve as junctions for the dynamic exchange reaction.[9] However, such systems are limited by the inherent drawbacks of metal salts: 1) Low solubilities of inorganic powders in epoxy resins require additional efforts for mixing, and 2) A high catalyst loading (>5%) is required, resulting in detrimental effects on material integrities and mechanical properties. Hence, a novel miscible catalyst that can accelerate the dynamic exchange reaction in epoxy vitrimer is necessary.

J.-H. Shin, M.-B. Yi, T.-H. Lee, H.-J. Kim
Department of Agriculture, Forestry and Bioresources
Seoul National University
Gwanak-ro 1, Gwanak-gu, Seoul 08826, Republic of Korea
E-mail: hjokim@snu.ac.kr
H.-J. Kim
Research Institute of Agriculture and Life Sciences
Seoul National University
Gwanak-ro 1, Gwanak-gu, Seoul 08826, Republic of Korea

The ORCID identification number(s) for the author(s) of this article can be found under https://doi.org/10.1002/adfm.202207329.

**ADVANCED
SCIENCE NEWS**
www.advancedsciencenews.com

**ADVANCED
FUNCTIONAL
MATERIALS**
www.afm-journal.de

Herein, a relatively novel molten-metal complex, a so-called solvate ionic liquid (SIL), was used as an additive to address previous catalysts' shortcomings simultaneously. The term SIL, introduced by Angell et al.,[10] refers to a system of oligoethers (glymes) and metal salts, which are coupled via coordination to form a new independent complex [M(glyme)]+. This multidentate sequestration facilitated by the neutral glyme (a Lewis base) enables the dissolution of metals into a liquid medium. Within the subcategories of ionic liquids, SILs feature remarkable properties such as non-flammability, negligible vapor pressure, and a low melting point (<100 °C); therefore, some species remain as liquids even at room temperature.[11] Moreover, owing to their high ionic mobilities, these compounds have been used as a reaction media in many reactions, including epoxy curing,[12] Diels–Alder reactions, and [2 + 2] diene cycloaddition.[13] Lastly, the versatility of SIL compositions can be an advantage, as the physicochemical properties and reactivities of such complexes can be readily tailored by modifying the combinations of metal cations, solvates, and anion types.[14]

Herein, a SIL composition was chosen such that it exhibited activities for both epoxy curing and dynamic exchange reaction. Metal acetoacetates had been previously proven to be effective in epoxy curing by Zhang and Wong.[15] The ability of the metal ions to coordinate with the epoxide depends strongly on the groups to which they belong, resulting in a significant variation in curing reactivities. Herein, lithium (alkali metal, monovalent), magnesium (alkaline earth metal, divalent), and zinc (transition metal, filled d^{10}) cations, with zero crystal-field stabilization energies (e.g., facile exchange of ligands with their surroundings) were employed. Two commonly used anions, trifluoromethanesulfonate (OTf-) and bis(trifluoromethanesulphonyl) imide (TFSI-), whose negative charges are strongly delocalized

via sulfur flanking groups and are hence mobile,[14] were selected. The hydrophobicity of the anions was also expected to impart air and moisture resistivities to the SIL. Triglyme (G3) was selected as the solvate for the lithium salts because of the compatibility of the ionic radius of Li+ and the cavity size of G3, and the resultant stability of the solvated structure.[16] Furthermore, tetraglyme (G4) was selected for the zinc and magnesium salts, owing to their higher charge densities. Using these combinations, we also aimed to maximize the stress-relaxation performance of a vinylogous urethane-based epoxy vitrimer. To the best of our knowledge, there have been few reports on magnesium and zinc-based SILs,[17] and this is the first report on the application of SILs to a vitrimer system. The objectives of using the SILs were as follows: 1) Elimination of metal-salt mixing processes that may induce unwanted pre-gelation or compromise mechanical strengths, 2) Enhancement of the catalytic activity of the metal cations during epoxy curing, and 3) Acceleration of the dynamic exchange reaction in cured vitrimer epoxy with a minimum catalyst dose (**Figure 1**).

A practical epoxy vitrimer system was designed by referring to a recent study by Spiesschaert et al., who introduced a vinylogous urethane (VU) platform into a commercial epoxy resin, wherein the dynamic exchange moieties were covalently bonded to the epoxides via epoxy-amine addition reactions.[18] By adjusting the SIL dosage in the resin formulation, vitrimer epoxy systems with tailored stress-relaxation capabilities were fabricated. Moreover, we aimed to use the material as a soft encapsulant for flexible electronics packaging. Developments for a deformable but tenacious material have been the desire of electronics industries, while a selection of material inevitably accompanies opportunity costs. Silicone-based elastomers (polydimethylsiloxane, PDMS) are the most frequently adopted
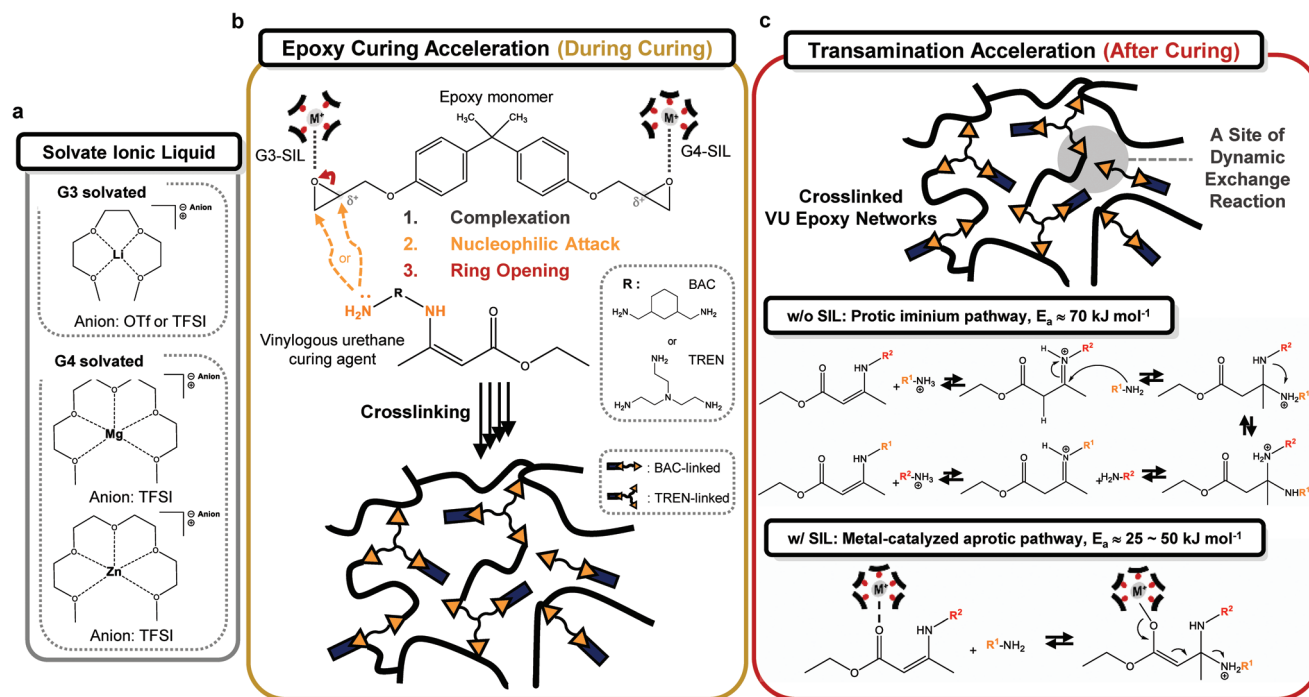

Figure 1. a) Chemical structures of solvate ionic liquids (SIL). b) The epoxy monomer, vinylogous urethane curing agent, as well as the schematic illustration of the SIL's functioning on epoxy curing reactions c) and dynamic exchange reactions.

**ADVANCED
SCIENCE NEWS**

www.advancedsciencenews.com

**ADVANCED
FUNCTIONAL
MATERIALS**

www.afm-journal.de

material for encapsulating flexible hybrid electronics (FHE);[19] however, they suffer from a lack of long-term stabilities caused by the properties such as mechanical endurance and gas or water vapor tightness.[20] In particular, the weak adhesion of PDMS to polyimide substrates (peel strength < 0.1 N mm^{-1})[21] can cause delamination and damage the FHEs during or after deformation.[22] In contrast, our epoxy-based encapsulant exhibited excellent adhesion over 100 bending or twisting cycles while maintaining its structural integrity due to the stress-relaxation and self-healing abilities of the vitrimer. We demonstrated, for the first time, the preparation of a vitrimer epoxy-supported soft encapsulation for a flexible substrate, simultaneously achieving a bendable encapsulation, warpage attenuation of the electronics package, and selective removal of the encapsulant after use.

2. Results and Discussion

2.1. Characterization of the Synthesized SILs

The synthesized G3 and G4-solvated SILs had structures similar to those reported in previous crystallographic and spectroscopic studies,[23] despite the differences in anion types (**Figure 2**a). In the G3-SILs, the core Li$^+$ was coordinated with four adjacent ethylene oxides and an oxygen atom from the SO$_2$ group of the TFSI anion, forming a 12-crown-4 ether-like coordination geometry.[23a,24] In the G4-SILs, the core Mg^{2+} or Zn^{2+} were coordinated with five adjacent ethylene oxides and an oxygen atom from the SO$_2$ group of the TFSI anion, forming a 15-crown-5 ether-like coordination geometry.[23b,25] The synthesized G3- and G4-solvated SILs ([Li(G3)]TFSI, [Li(G3)]OTf, [Mg$_{0.5}$(G4)]TFSI, and [Zn$_{0.5}$(G4)]TFSI) remained as homogeneous liquids even after being cooled to room temperature, and no phase separation was observed (Figure 2b). The SILs exhibited broad melt-temperature (T$_m$) ranges of 0–30 °C (Figure S4, Supporting Information) and dynamic viscosities between 250 and 13000 mPa s at 25 °C (Table S1, Supporting Information), demonstrating Arrhenius depletion as a function of temperature (Figure S5, Supporting Information). Next, the chemical natures and coordination states of the SILs were studied using Infrared (IR) and Raman spectroscopy (Figure 2c,e). The spectra of the SILs proved that the complexation between the molten-metal cation and glymes had been successful (see details in the Supporting Information). Finally, the thermal stabilities of the SILs were investigated to account for the working conditions of vitrimer epoxy (Figure 2f). All the SILs showed a significantly higher T$_{d5\%}$ value (>180 °C) than those for pure G3 and G4 (≈110 °C), owing to metal-glyme complexation, confirming their stabilities as additives in both epoxy processing and use.

2.2. Rapid Curing by the Introduction of SILs

Recently, lithium-based SILs have been reportedly used in epoxy curing reactions with a significant decrease and increase in curing temperature and rate, respectively.[12,26] Encouraged
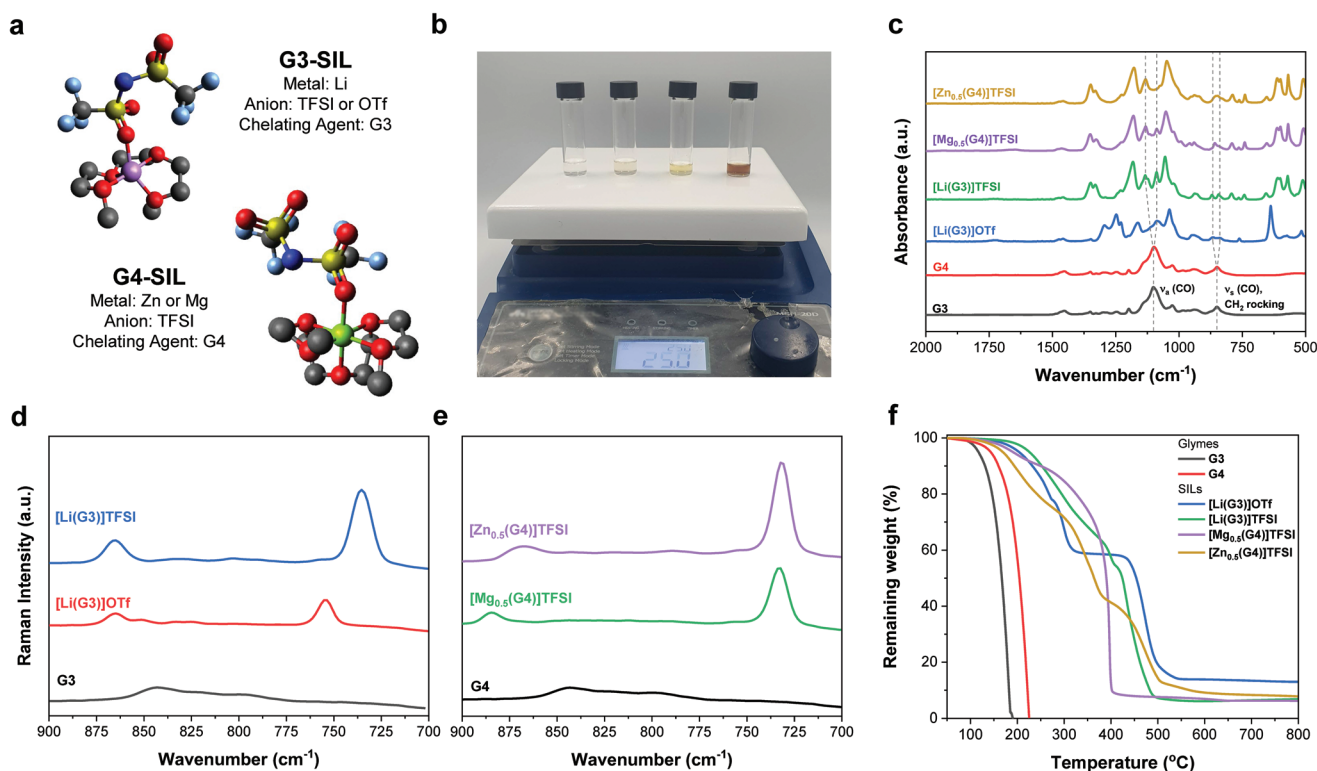

Figure 2. a) Geometrically optimized representative solvate structures of G3-solvated SIL (top) and G4-solvated SIL (bottom); H atoms have been omitted for clarity; Purple, Li; Green, Zn or Mg; Red, O; Black, C; Blue, N; Yellow, S; Azure, F. b) The synthesized SILs (left to right): [Li(G3)]OTf, [Li(G3)]TFSI, [Mg$_{0.5}$(G4)]TFSI, and [Zn$_{0.5}$(G4)]TFSI. c) The attenuated total reflection infrared (ATR-IR) spectra of the glymes and SILs. d) The Raman spectra of G3 and G3-based SILs and e) G4 and G4-based SILs between 700 and 900 cm^{-1}. f) The thermal degradation curves of the glymes and SILs from 40 to 800 °C.
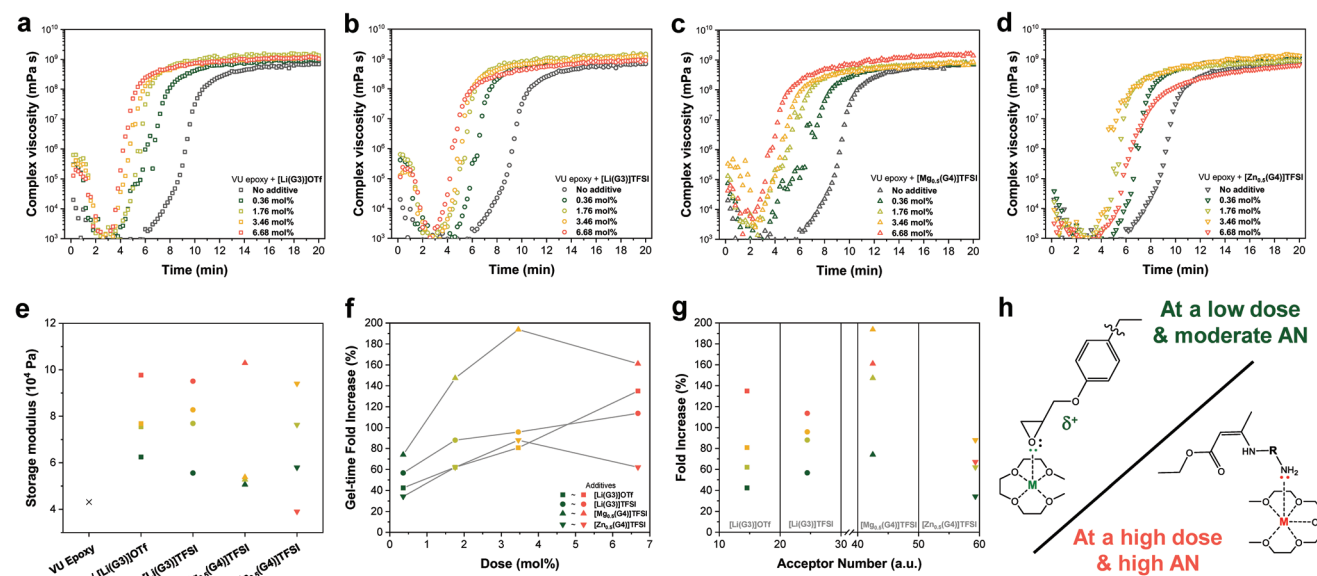
Figure 3. a–d) Viscosity profiles of a stoichiometric VU epoxy mixture containing [Li(G3)]OTf, [Li(G3)]TFSI, [Mg$_{0.5}$(G4)]TFSI, and [Zn$_{0.5}$(G4)]TFSI, respectively, as a function of dosage (0–6.68 mol%). e) Storage modulus of the cured-VU-epoxies containing SILs after 20 min (green, 0.36 mol%; pale green, 1.76 mol%; orange, 3.46 mol%; and red, 6.68 mol%). f) The effect of the additives on gel-time as a function of dosage. g) The effect of additives on gel-time as a function of the Gutmann AN. h) The proposed Lewis acidic interaction of the SIL; with (left) a moderate AN, activating the epoxide moiety at a low dose or (right) of a high AN, deactivating amine species at a high dose.

by these results, we examined the curing behaviors of vitrimer epoxy systems consisting of diglycidyl ether of bisphenol A (DGEBA) epoxy and VU-containing curing agents (VU CA) with various additives, using a rheometer. All the SIL-loaded mixtures readily become homogenous at room temperature with minimum stirring. Initially, a reference VU Epoxy without additive was cured at 120 °C (**Figure 3**). The reaction started after 7.6 min, indicated by an initial viscosity rise (onset time, Table S3, Supporting Information), while its gel point—the point of crossover of the storage and loss moduli (G' = G'')—was determined to be 9.4 min (Figure S11, Supporting Information). With the addition of 1.76 mol% of Zn(OAc)$_2$ to the system, no acceleration was observed (Figure S12, Supporting Information).

In contrast, all the other SILs exhibited excellent curing accelerating abilities, recording substantial reductions in both onset and gel-time. Upon addition of only 0.36 mol% of [Li(G3)]OTf, the gel time was reduced by ≈30% (Figure 3a; Table S3, Supporting Information). Further improvements were observed by increasing the doses of the SIL to 1.76, 3.76, and 6.68 mol% in the VU epoxy mixture. The positive correlations between the SIL dosage and increase in cure rate were also consistently observed in the cases of using Li-cored SILs (Figure 3a,b). At 6.68 mol% of [Li(G3)]TFSI, the onset and gel crossover time were reduced to 3.8 and 4.4 min, respectively (Figure 3b; Figure S14, Supporting Information), which was equivalent to a 53% reduction (also equivalent to a 116% fold increase in the curing rate) over the pure VU epoxy system. The curing acceleration effect was further enhanced by adopting the Mg-cored SIL (Figure 3c). At 3.46 mol% of [Mg$_{0.5}$(G4)]TFSI, the onset and gel crossover time were even reduced to 3.0 and 3.2 min, respectively (Figure 3c; Figure S15, Supporting Information). Hameed et al. obtained a similar tendency of increasing epoxy cure rate with the addition of Li- or Mg-cored SILs, which they ascribed

to the following reasons: 1) A reduction in the glass transition temperature (T$_g$) of resin mixtures (e.g., plasticization), and 2) The Lewis-acid activation of the epoxide moiety via lithium-to-oxirane coordination.[12] In our study, the reduction in T$_g$ upon SIL addition was not significant; however, the complexation of the molten-metal ion to the O-ligand of the epoxides was indicated by the IR analyses (Figure S17, Supporting Information). The intensities of the characteristic bands assigned to epoxide gradually decreased as the SILs were mixed with the uncured epoxy resin; symmetric breathing, asymmetric vibration, and symmetric vibration modes were observed at 1228, 913, and 825 cm^{-1}, respectively. The damped vibrational signal of the epoxide C−O bond confirmed the complexation. While both the terminal and benzylic carbons could be a target of aliphatic VU CA (Figure S20, Supporting Information), the coordination of SIL induced the more substituted α-carbon of an epoxide to have a cationic character, and hence, to be more susceptible to nucleophilic (Table S4, Supporting Information). Similar behavior of epoxides has been reported when using Lewis acids as a catalyst.[27] We speculate that there had been a sequential complexation, facilitated ring-opening, and curing reaction in concert with the nucleophilic addition of neighboring amine moieties in our SIL-containing epoxy during network formation (Figure 1b). Hence, we surmised that the catalytic effect relied strongly on the polarization of the epoxide C−O bond (basicity) and the Lewis acidity of the SILs used. Therefore, we employed the quantitative Gutmann acceptor number (AN) to predict the probability of coordination between the compound and its surroundings,[14,28] representing the SIL's electrochemical properties.[13] To examine the effectiveness of the parameter for gelation, the cure rate fold increase was plotted against the AN of the SILs, pre-determined by the Gutmann procedure[29] (Figure 3g; Table S2, Supporting Information). The ANs of

the lithium-cored SILs were correlated with the resultant fold increase, suggesting that the Lewis acidity of additives was a dominant factor in determining the formation of O-ligand/Metal complexes and accelerating the epoxy ring-opening reactions.

In contrast, [Mg$_{0.5}$(G4)]TFSI and [Zn$_{0.5}$(G4)]TFSI initially exhibited a gradual reduction in the gel time with increasing dosage and followed the dosage–cure rate relationship (Figure 3c,d). By 3.46 mol% addition of [Zn$_{0.5}$(G4)]TFSI, the onset and gel crossover times were consistently reduced to 4.4 and 5.0 min, respectively (Figure 3d; Figures S15 and S16, Supporting Information). However, the addition of 6.68 mol% each of [Mg$_{0.5}$(G4)]TFSI and [Zn$_{0.5}$(G4)]TFSI to the VU epoxy mixture increased the fold rate by 161% and 67%, respectively, whereas the addition of 3.46 mol% each of [Mg$_{0.5}$(G4)]TFSI and [Zn$_{0.5}$(G4)]TFSI increased it by 194% and 88%, respectively (Figure 3f). Notably, the rate of cure-rate acceleration from 3.46 to 6.68 mol% dosages progressively decreased as a function of the AN. At the higher dosage, the SIL with a higher AN formed a complex with not only the epoxides, but also the amino species in VU CA, which had not been favored before. This deprived the ligating nitrogen of electron lone pairs (N-ligand/metal), and its basicity toward the epoxides was reduced, resulting in an attenuated curing reaction. A similar result had been previously observed by Omrani et al., wherein the amino groups were deactivated to prepare a latent curing epoxy system.[30] The IR analyses were repeated with the mixture of VU CA and the used additives (Figure S18, Supporting Information) to demonstrate the complexation that occurred with the addition of those SILs (see details in the Supporting Information). These findings show that the interaction of SILs with ligating candidates depends on the abundance and Lewis acidity of the SILs, which determines their accessibility to surrounding viable moieties.

2.3. Accelerations on Transamination by the Incorporation of SILs (Model Study)

We further explored the catalytic activity of the synthesized SILs toward transamination using a simple model system, referring to a previous study by Denissen et al.[31] A fivefold excess of the VU model compound (R1) versus 2-ethylhexylamine (R2) was employed with a small dose of additives (**Figure 4**a). Hence, the lower limit of the [R1] fraction at the point of [R2] depletion is 0.8. The reaction was performed at 70 °C, a reasonably low temperature for a vinylogous urethane-based system with a typical reaction temperature over 120 °C, to suppress side reactions and evaporation. Proton transfers between protonated primary amines (in R2) and secondary amines (in R1) are known to play an essential role in cases, where the presence of Lewis acids significantly increases the reaction rate.[31] First, a zinc acetate salt, the most prominent catalyst for various dynamic exchange reaction systems,[4a,b,9a] was analyzed as the reference additive. In the zinc-catalyzed transesterification system, Zn^{2+}-chelated carbonyl or carboxyl functionalities increase the partial charge on sp^3 carbon atoms.[4b] Analogously, the $Zn(OAc)_2$ was expected to have a similar catalytic effect in the transamination reaction. With the use of 2 mol% (vs [R1]) of $Zn(OAc)_2$, a reaction rate higher than that without the catalyst was obtained (Figure 4b). However, the system did not reach equilibrium even after 60 min, even though the catalyst loading
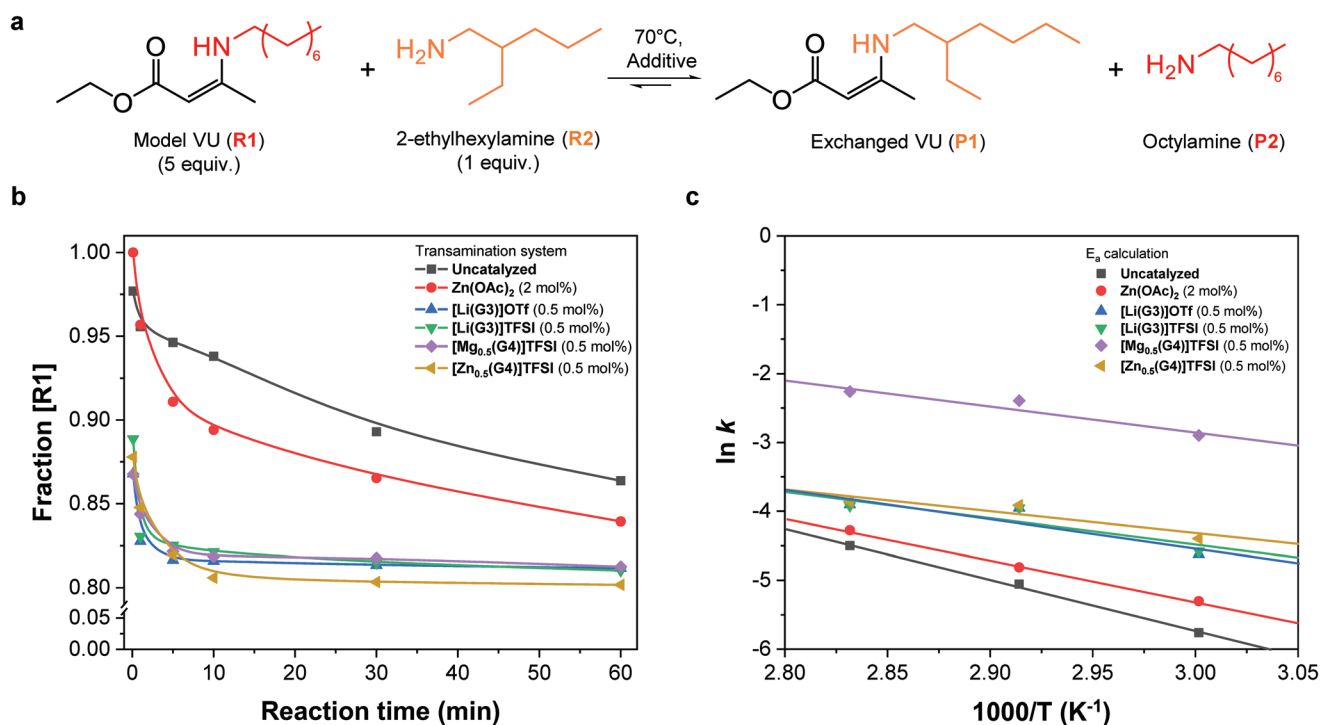

Figure 4. a) Model transamination reaction between a model VU compound (R1) and 2-ethylhexylamine (R2). b) Decrease in model VU as a function of time at 70 °C in the presence of various additives, reaching equilibrium for a fraction of remaining R1 of ≈0.8. The amount of catalyst was calculated as mol% versus R2. c) Arrhenius plot of the resultant kinetics.

**ADVANCED
SCIENCE NEWS**

www.advancedsciencenews.com

**ADVANCED
FUNCTIONAL
MATERIALS**

www.afm-journal.de

Table 1. Overview of the activation energies from the model study and stress relaxation experiments of all the VU epoxies with and without additives.

Catalysts	E_a from model study [kJ mol^{-1}]	E_a from stress-relaxation [kJ mol^{-1}]
Uncatalyzed	62 ± 3	71 ± 4
Zn(OAc)$_2$ (1 mol%)	50 ± 2	70 ± 18
[Li(G3)]OTf (0.5 mol%)	35 ± 17	47 ± 6
[Li(G3)]TFSI (0.5 mol%)	32 ± 16	47 ± 3
[Mg$_{0.5}$(G4)]TFSI (0.5 mol%)	31 ± 10	39 ± 3
[Mg$_{0.5}$(G4)]TFSI (2 mol%)	–	24 ± 5
[Zn$_{0.5}$(G4)]TFSI (0.5 mol%)	26 ± 12	39 ± 2
[Zn$_{0.5}$(G4)]TFSI (2 mol%)	–	27 ± 4

(2 mol%) was fourfold that of other additives, which was attributed to its poor solubility in the medium. Denissen et al. also reported similar results with sulphuric acid being, which had been found to be less efficient than other organocatalysts due to low solubility. Considering this, it is noteworthy that the SIL-introduced systems exhibited much higher reaction rates and reached equilibrium rapidly (<10 min), despite lower catalyst dosages (0.5 mol%). The glyme-solvated compounds were miscible with the liquid media, enabling the system to fully utilize the high proton transfer ability of metal cations.

The model study exhibited pseudo-first-order linear decay kinetics at low conversions and reached an equilibrium plateau (Figure 4b). The kinetic curves showed the temperature dependence of typical dynamic exchange reactions (Figures S22 and S23, Supporting Information). The first few points were fitted to the Arrhenius equation to determine the initial rates of the conversion and calculate the activation energies (Figure 4c and **Table 1**). Subsequently, an activation energy of 62 ± 3 kJ mol^{-1} was calculated for the transamination of the uncatalyzed VU model system, which is consistent with previous reports (59–73 kJ mol^{-1}).[5b,6a,31] According to calculations by Du Prez et al. for vinylogous urethanes, our model system proceeded via a protic iminium pathway, even though no additive had been used; whereas markedly different temperature dependences were observed in systems with additives. The activation energy of the Zn(OAc)$_2$-added system was ≈50 kJ mol^{-1}, indicating a slight catalytic effect. Furthermore, the SIL-loaded systems resulted in significant reductions in the enthalpic barriers (E_a), which were reduced to almost half that of the uncatalyzed system. Denissen et al. also reported an acid-catalyzed transamination system with an activation energy of 47 kJ mol^{-1}, attributing it to a shift in the reaction pathway to a more direct one.[31] In our study, the G4-solvated multivalent SILs recorded particularly low activation energies; 31 and 26 kJ mol^{-1} for the systems with [Mg$_{0.5}$(G4)]TFSI and [Zn$_{0.5}$(G4)]TFSI, respectively. Since no Brønsted acid or protic solvent was involved in the system, the exchange reaction may not have followed the accelerated protic imine metathesis pathway dominated by the active protonated amine or imine species.[6a] Instead, the reaction is believed to commence with a metal complexation similar to Michael addition, following the activation of the carbonyl sites of vinylogous urethanes, which stabilized the resultant

zwitterionic intermediates via conjugation. Moreover, the degree of reduction in activation energies matches the order of the Gutmann AN of each SIL, indicating that the ability of the additive to accept electron pairs strongly influenced the carbonyl complexation, which will be discussed using IR data in Section 2.4.

2.4. Accelerations on Transamination by the Incorporation of SILs (VU Epoxy Networks)

Having verified the potency of the SILs on the model compounds, we explored their effects on the cured VU epoxy networks as well. VU epoxy networks were prepared according to the adapted ratio with a 5% excess of the primary amines (no extrusion of SIL from the cured epoxy was observed, Figure S29, Supporting Information). After the curing schedule, glassy elastic moduli (>10^9 Pa @ 25 °C, Figure S25, Supporting Information) and thermal stabilities (<1.5% mass loss at 150 °C for 1 h, Figure S24, Supporting Information, <3% mass loss after burn-in test, Table S7, Supporting Information) were obtained for all the systems, with or without additives. For the tensile tests, dog-bone-shaped specimens of the VU epoxies with and without additives (0.5 mol%), having clean and homogeneous appearances (except for the specimen with Zn(OAc)$_2$ powder), were fabricated (Figure S26, Supporting Information). The representative stress–strain curves obtained at room temperature and 80 °C are shown in **Figure 5**, and their mechanical properties are summarized in **Table 2**. Notably, a small loading of Zn(OAc)$_2$ substantially reduced the tensile strength (30 MPa) at room temperature, which was less than half that of the reference VU Epoxy (69 MPa). This was ascribed to the fact that the interphase between the epoxy matrix and metal powder was vulnerable to the propagation of cracks throughout the composite. In contrast, with the use of SILs as additives (0.5 mol%), the continuous networks yielded significantly higher tensile strengths (>50 MPa) at room temperature. As stated in Section 2.2, the SILs had advantageous effects on the final storage moduli of cured VU epoxies (Figure 3e), which appeared to compensate for the T_g-reduction effects (Table 2) on the tensile strength. At 80 °C, all SIL-containing VU epoxies exhibited similar or higher elongations (30–40%) than those obtained in the uncatalyzed and Zn(OAc)$_2$-catalyzed samples. These results demonstrate the potential of SIL-containing VU epoxies as engineering materials and their ability to achieve excellent properties in both target temperatures.

Next, the dynamic nature of VU epoxies, especially the potency of the SILs, was examined via stress-relaxation experiments (**Figure 6**). The stress-relaxation behavior of the VU epoxy followed the Maxwell model, resulting from the percolation of dynamic reversible bonds to the system (Figure 6a).[32] With an increase in the temperature from 130 to 160 °C, the relaxation time (τ^*) decreased according to Arrhenius law for all VU epoxies with or without the additive (Figure S28, Supporting Information). This is consistent with previously reported epoxy vitrimer systems.[31,33] The relaxation curves from the catalyzed system at 140 °C have been compared in Figure 6b. While the reference network showed a τ^* of 2000 s, it was reduced to 1500 s with the addition of 2 mol% Zn(OAc)$_2$, as stated in the previous report.[4b] With SILs as catalyst (0.5 mol%), the τ^* was
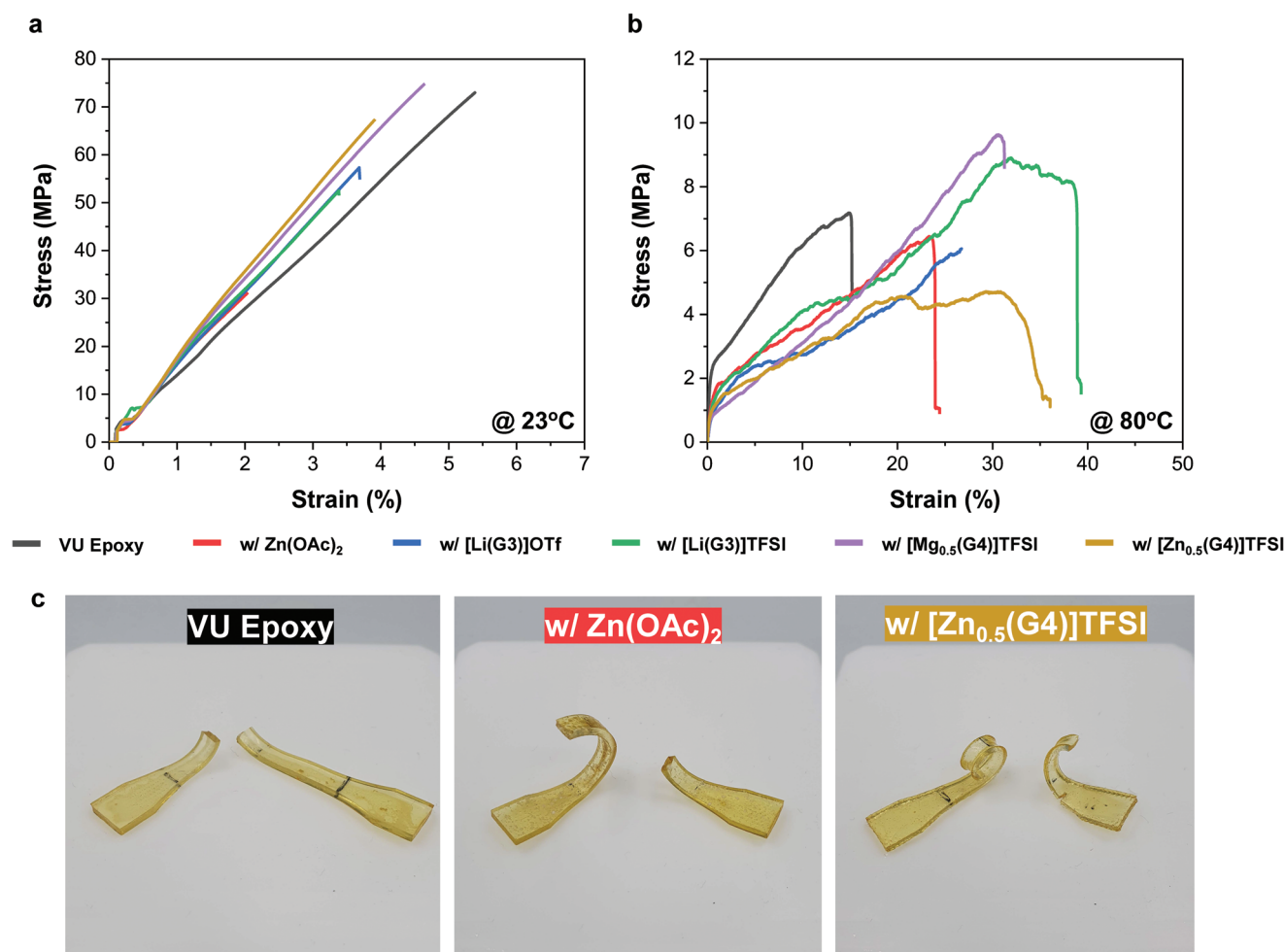
Figure 5. Representative strain–stress curves of the cured VU Epoxies with or without SILs; measured at a) 23 and b) 80 °C. c) Broken VU Epoxy specimen without additive, with $Zn(OAc)_2$, and with $[Zn_{0.5}(G4)]TFSI$ after the tensile test at 80 °C.

further reduced to 1000 s ([Li(G3)]OTf), 462 s ([Mg_{0.5}(G4)]TFSI), 405 s ([Li(G3)]TFSI), and 344 s ([Zn_{0.5}(G4)]TFSI). The result denotes that the SILs have substantially better catalytic activities for transamination in a VU network than $Zn(OAc)_2$. While the catalytic activity did not follow a linear order, its effect differed with the type of metal and counter anion, as indicated by the model study. To further explore the effect, VU epoxies with a higher dosage of the SILs (2 mol%) were fabricated and tested at 160 °C (Figure 6c). Remarkably, an increment in dose accelerated the dynamic exchange reaction further, resulting in τ^* of 19 s and 26 s for systems containing 2 mol% each of [Mg_{0.5}(G4)] TFSI and [Zn_{0.5}(G4)]TFSI, respectively. To date, a better external catalyst with this low dosage has not been reported for vitrimer epoxy systems. Considering that there was no compositional change from the reference VU epoxy (with a τ^* of 730 s at 160 °C), this tremendous acceleration (≈38 or 28-fold, respectively) could be solely attributed to the catalytic effect of the SILs. As no significant difference in the T_g or storage and loss moduli was observed within the temperature range (Table 2; Figure S25, Supporting Information), the acceleration was concluded not to have originated from rheological differences such as chain mobility or cross-linking density.

From the relaxation times, obtained at various temperatures, a linear relationship between $\ln(\tau^*)$ and 1000/T was fitted to the Arrhenius plot (Figure 6d). The corresponding activation energies were calculated from the slopes. The measured activation energies of the reference VU Epoxy and $Zn(OAc)_2$-catalyzed system were 71 ± 4 and 70 ± 18 kJ mol⁻¹, respectively, which are consistent with those for the transamination system via a neutral iminium pathway.[31] With the addition of the SILs, the systems exhibited apparent downward shifts in $\ln(\tau^*)$ and slow grades in the corresponding slopes, yielding significantly lower activation energies even below 50 kJ mol⁻¹, as listed in Table 1. The activation energies obtained from a model study and a stress-relaxation test were almost equal; however, a rise in the absolute values was observed for the latter. Since all systems, with or without additives, shared the same ratio of the free primary amines and VU secondary amines, there appeared to be a significant change in a reaction pathway due to the SIL. Denissen et al. reported a metal-catalyzed pathway using 1.9 mol% of dibutyltin dilaurate as an additive, reducing the thermal barrier of the transamination reaction to only 30 kJ mol⁻¹.[31] In our system, the molten-metal cations of SILs were expected to similarly serve as Lewis acids and form O-ligand/Metal

Table 2. Thermal and mechanical properties of the VU epoxies with and without additives.

Entry	Dose [mol%]	$T_{d5\%}$ [°C]	T_g [°C]	$\tau^*_{160\,°C}$ [s]	ε at 25 °C [%]	ε at 80 °C [%]	σ at 25 °C [MPa]	σ at 80 °C [MPa]
VU Epoxy	0	259	66.2	730	5.3 (±0.6)	15.0 (±2.9)	68.7 (±8.2)	8.5 (±2.0)
w/ Zn(OAc)$_2$	0.5	260	68.2	757	3.2 (±1.1)	29.7 (±4.1)	29.8 (±3.6)	8.4 (±1.8)
	2	–	62.8	–	–	–	–	–
w/ [Li(G3)]OTf	0.5	267	64.3	487	3.8 (±0.6)	27.0 (±4.0)	55.8 (±3.9)	6.1 (±0.5)
w/ [Li(G3)]TFSI	0.5	252	65.6	217	3.6 (±0.8)	43.2 (±2.3)	46.1 (±3.6)	8.3 (±1.2)
w/ [Mg$_{0.5}$(G4)]TFSI	0.5	251	64.5	255	4.1 (±0.6)	25.1 (±3.4)	56.4 (±10.0)	7.5 (±1.5)
	2	–	61	19	–	–	–	–
w/ [Zn$_{0.5}$(G4)]TFSI	0.5	259	63.3	213	4.1 (±0.5)	30.8 (±2.7)	55.7 (±9.4)	5.9 (±0.3)
	2	–	61.6	26	–	–	–	–

complexes with the oxygen atom in the carbonyl groups within the VU Epoxy system. With the addition of the SILs to the VU CA medium, the intensity of the characteristic IR band at 1645 cm^{-1}, corresponding to the carbonyl stretching vibration, decreased gradually as a function of dosage (0–5 mol%), owing to metal-coordination (Figure S18, Supporting Information). A similar shift was also reportedly observed in the VU acrylate system with the addition of zinc chloride.[5c] In those IR spectra, reductions in the intensities of the absorbance bands, ascribed to −NH$_2$, were also observed, indicating coordination of the SILs with the primary amine species. In concert with the deactivation of the protonated amine species, the reaction further diverged from the original protic iminium pathway and followed the metal-catalyzed mechanism with a significantly lower enthalpic barrier. This metal-catalyzed transamination pathway, previously unidentified, probably due to the low solubility of metal salts in the medium, demonstrated excellent efficacy for the VU dynamic exchange reaction, owing to the facile introduction of SILs into the vitrimer-resin mixture.

2.5. Fabrication of a Soft Encapsulation on Flexible Printed Circuit Board

To demonstrate the potential of stress-relaxable vitrimer epoxies for soft encapsulation techniques accessing flexible, bendable, or undevelopable surfaces, a simple layered electronics package composed of an encapsulant, an IC chip, and a flexible printed circuit board (FPCB) was fabricated, and integrated via routine epoxy coating and curing (**Figure 7**a). Three types of testing specimens were fabricated using various encapsulants: A normal epoxy (cured with the same curing agent composition, except without exchangeable moieties) with no activity toward dynamic exchange reactions, PDMS (SYLGARD™ 184) as the reference soft encapsulant, and a vitrimer epoxy containing 2 mol% of [Zn0.5(G4)]TFSI. Figure 7b shows the prepared bending-test specimen. The bending set experiments involved the following

processes: 1) Both sides of the specimen, attached to the fixed and moving stages, were stretched. 2) The specimen was bent into an arc by pushing the moving stage using a pendulum (500 g) and held at the new position. 3) The specimen reverted to the relaxed state after removing the pendulum (Figure 7c). The heating plate at the bottom plane during the experiment was maintained at 100 °C to facilitate topology rearrangement. Notably, the specimen capped with the vitrimer epoxy bent significantly under pressure and yielded a radius curvature of 2.5 cm from the baseline (Figures 7c and 2). At this stage, close-up images of the deformed plane of each specimen exhibited definite differences in their reaction to compression (Figure 7d). A specimen capped with the normal epoxy could not be retracted or deformed due to its high storage modulus, which is generally anticipated for the material. Only the edge of the polyimide strip, where no encapsulant had been applied, folded perpendicularly to the capped plane. The PDMS-capped specimen was readily deformed as expected. However, there was a critical adhesive failure at the interface between the PI substrate and the encapsulant, owing to its low effective modulus and weak adhesion. In contrast, the specimen capped with the vitrimer epoxy conformed to the compression without adhesion failure, exhibiting a perfect encapsulation performance even in the curved state. Furthermore, the retracting/bending movements can be modulated manually (Video S1, Supporting Information). This remarkable bendability was attributed to the rapid dynamic exchange reaction and supreme stress-relaxation capabilities of the vitrimer epoxy encapsulant, which made the encapsulation approach compatible with complex geometries without causing severe stress buildup at the interface. Further, the vitrimer epoxy with SIL (2 mol% of [Zn$_{0.5}$(G4)]TFSI) even survived 100 cycles of bending and twisting tests without damage (Figures S30 and S31, Supporting Information). The fast stress-relaxation afforded macroscopic topology rearrangements multiple times, which are required to accommodate the repeated elastic strain/stress of a polyimide substrate during the cyclic tests.

Next, we explored the warpage issue of the FPCB, followed by the encapsulation. During the curing and cooling of the
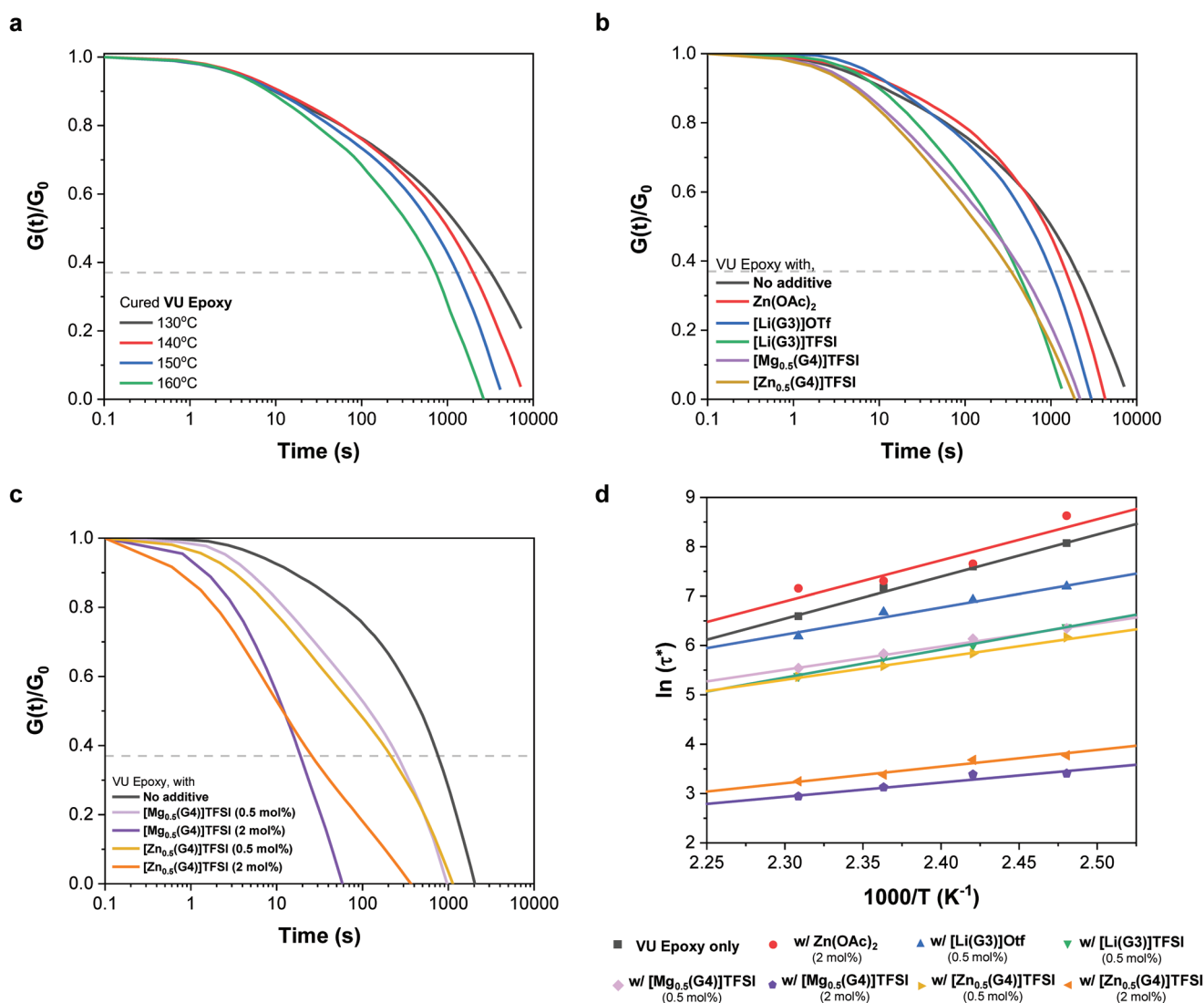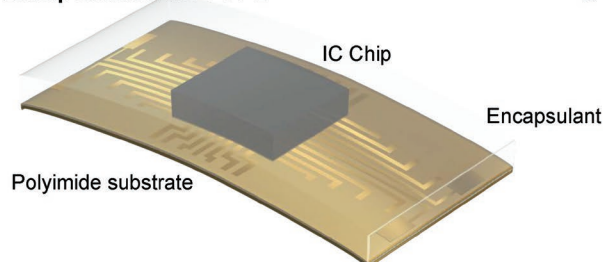
**ADVANCED
SCIENCE NEWS**

www.advancedsciencenews.com

**ADVANCED
FUNCTIONAL
MATERIALS**

www.afm-journal.de

Figure 6. Representative stress-relaxation and Arrhenius curves of VU Epoxies: a) Stress-relaxation curves of cured VU Epoxy between 130 and 160 °C. The dotted line represents $G(t)/G_0 = 1/e$, which defines the characteristic relaxation time (τ^*). b) Stress-relaxation curves of VU Epoxies without additive (black), with 2 mol% of $Zn(OAc)_2$ (red), 0.5 mol% of [Li(G3)]OTf (blue), [Li(G3)]TFSI (green), [Mg$_{0.5}$(G4)]TFSI (magenta), and [Zn$_{0.5}$(G4)]TFSI (brown) at 140 °C. c) Stress-relaxation curves of VU Epoxies containing [Mg$_{0.5}$(G4)]TFSI and [Zn$_{0.5}$(G4)]TFSI as a function of dosage: 0.5 or 2 mol% at 160 °C. d) Arrhenius curves of VU Epoxies containing various additives.
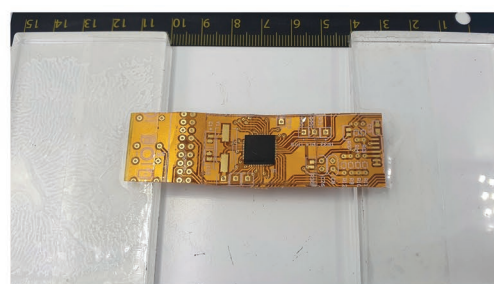
encapsulants, both the internal and interfacial shrinkage impact the layered multi-components, warping the most vulnerable part.[34] As shown in Figure 7e, the FPCB surface was randomly warped into an arbitrary shape; hence, the highest warped value was set as warpage and measured for the samples. The sample coated with the normal epoxy showed the highest warpage of 5.4 mm, whereas that with PDMS yielded much lower warpage of 1.6 mm due to the differences in cure shrinkage and the gap in the storage moduli. In this context, it is noteworthy that the sample containing the vitrimer epoxy recorded the lowest warpage of 1.5 mm, despite a high storage modulus (G' ≈10^9 Pa) of VU epoxy at room temperature. The warpage reduction was attributed to two factors: 1) The rearrangement of the vitrimer network at the curing temperature, which alleviated the cure-shrinkage-induced tension in the encapsulant, and 2) a gradual

increase in the storage modulus (G' ≈10^5–10^9 Pa) of the encapsulant during cooling, which prevented a coefficient of thermal expansion (CTE) or modulus mismatch-driven exfoliation along the interface of the encapsulant and PI substrate. Furthermore, the warpage was further reduced to 0.6 mm after a hot-pressing for 5 min at 100 °C, owing to the malleability of the vitrimer epoxy (Figure 7f). Finally, we demonstrated that it was able to selectively remove the encapsulant without damaging the chip interconnection and the printed circuits beneath. While heated at 160 °C, the softened encapsulant was scraped off, resulting in adhesive failure with a little residue. These findings can provide an innovative approach to simultaneously addressing the formability of materials, warpage issue of flexible substrates, and reusability of components, thereby raising manufacturing productivity and cutting costs.
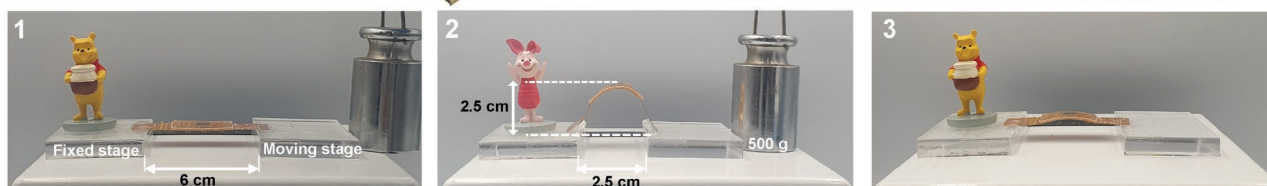
**ADVANCED
SCIENCE NEWS**

www.advancedsciencenews.com
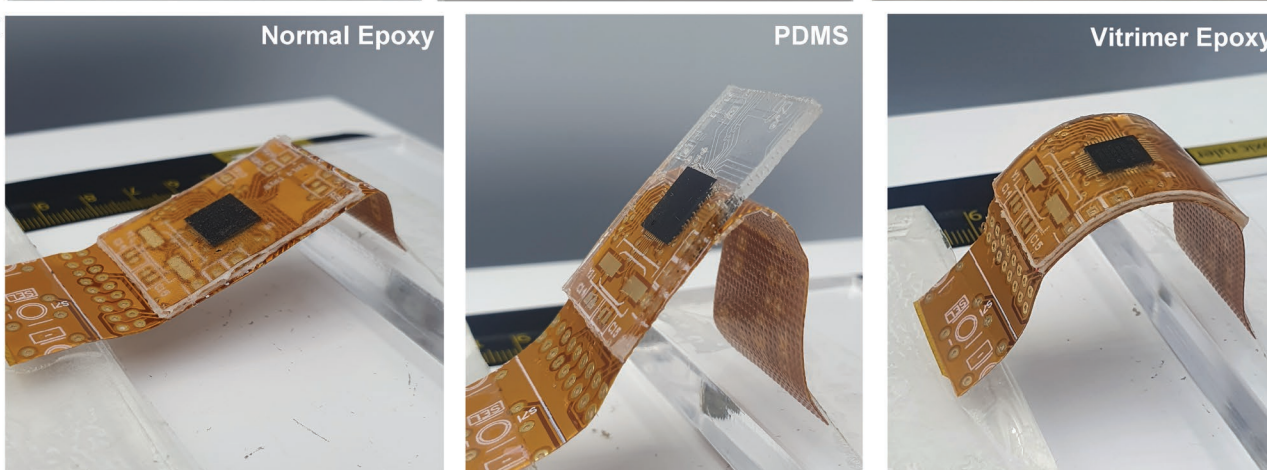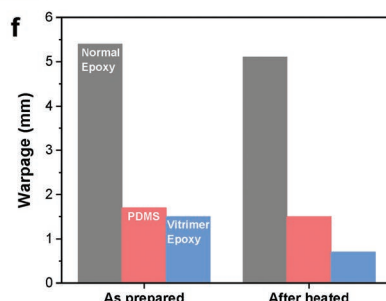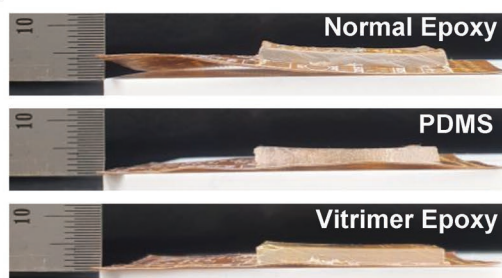
**ADVANCED
FUNCTIONAL
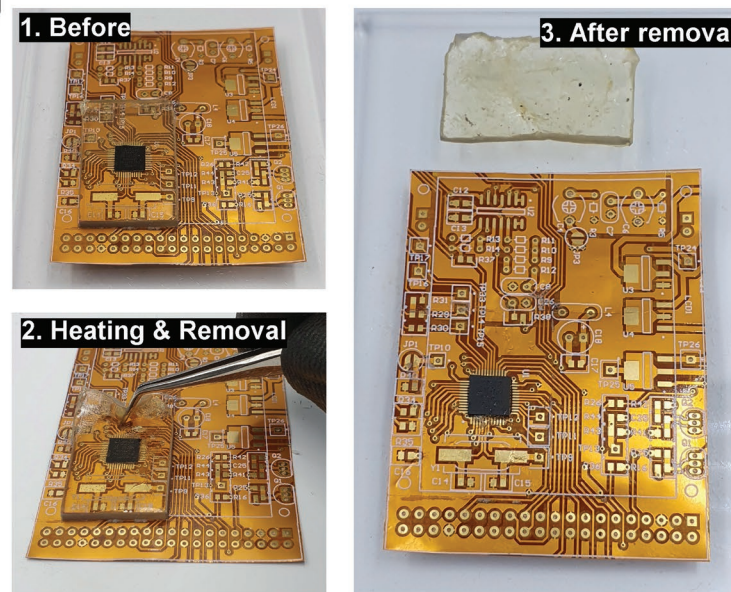MATERIALS**

www.afm-journal.de

Figure 7. a) Schematic representation of a miniaturized vitrimer epoxy-encapsulated FPCB. b) Top view of specimen layers with an encapsulant-IC chip-FPCB substrate. c) Bending test at 100 °C: 1) Before test; 2) Deformation by pushing a 500 g pendulum; 3) Relaxation by removing the pendulum. d) FPCBs using various encapsulants at the deformed state c2: (left) a normal epoxy, (middle) PDMS, and (right) vitrimer epoxy, exhibiting bending of the layers without adhesion failure. e) Warpage measurements of the as-prepared specimen using various encapsulants; f) The measured warpage before and after heating (100 °C). g) Reworkability test for the vitrimer epoxy-encapsulated specimen at 160 °C, demonstrating the encapsulant was cleanly removed without damaging the chip and substrate.

3. Conclusion

In summary, we demonstrated the fabrication of an electronic grade epoxy vitrimer using small loadings of various types of SILs. During epoxy curing, introducing SILs into a commercial epoxy/VU CA mixture accelerated epoxy ring-opening and amine-addition reactions, resulting in a drastic decrease in both the onset and gel-time, measured via rheological profiles. The catalytic performance was modulated by simply changing the dosage of the SILs. IR analyses revealed complex formation between the SILs and epoxides, which rendered a significant cationic character to the adjacent α- carbon, making it susceptible to nucleophilic attack by the neighboring amines, resulting in accelerated curing. We hypothesized that the Lewis acidity of the SIL, expressed via its Gutmann AN, would affect the degree of its catalytic activity and discovered that they were correlated. However, $[Zn_{0.5}(G4)]TFSI$, which had the highest AN, exhibited a more complex relationship at higher dosages. In those cases, the coordination bonds extended to the amino species, inhibiting their subsequent nucleophilic addition to epoxide.

The role of the SILs changed after the vitrimer epoxy had been fully cured, and they significantly accelerated the transamination reactions in the model compounds and within cross-linked epoxy networks. The molten-metal cations in SILs acted as Lewis acids, creating a direct carbonyl activation pathway and significantly reducing the enthalpic barriers for transamination reactions. Therefore, the prepared VU epoxies behaved like ordinary glassy epoxies at room temperature and exhibited complete stress-relaxation over a short time scale at higher temperatures. The tensile tests conducted at room temperature and 80 °C revealed that the SIL-containing samples retained their mechanical strength and showed higher elongations, outperforming both the uncatalyzed and the $Zn(OAc)_2$-containing VU epoxies. Thus, incorporating SILs into vitrimer epoxy facilitated rapid curing and stress relaxation in a moderate temperature range without diverging significantly from customary epoxy formulations, and thus, attributed to its broad applicability in the conventional epoxy-employing industries. Since the complexation of SILs for activating epoxide or carbonyl moieties requires no specific chemistry, we envisaged that the strategy should, in principle, apply to a broader range of epoxy curing or dynamic exchange systems.

Finally, the SIL-loaded epoxy vitrimer was successfully employed to fabricate a flexible hybrid electronics package capable of bending, warpage reduction, and rework, addressing the current issues in manufacturing industries. Further studies on the application of vitrimer epoxies in stress relaxation packaging may reveal their advantages over conventional thermosets and PDMS-based elastomers for stress relaxation, formability, reworkability, compatibility, and adhesion performance. In addition, such a technology could prevent wasting valuable electronic components, which would benefit the industry and the environment. Furthermore, as vitrimer epoxy is robust yet malleable, further studies are currently underway on its application as a coating material for undevelopable surfaces such as curved electronics.

Supporting Information

Supporting Information is available from the Wiley Online Library or from the author.

Conflict of Interest

The authors declare no conflict of interest.

Author Contributions

J. H. S. conceived the idea, designed and performed the experiments, analyzed the results, and wrote the original draft. M. B. L. and T. H. L. assisted the experiments and characterizations. H. J. K. reviewed and edited the original draft and supervised the research. All authors discussed the results and commented on the paper.

Data Availability Statement

The data that support the findings of this study are available from the corresponding author upon reasonable request.

[1] D. Montarnal, M. Capelot, F. Tournilhac, L. Leibler, *Science* **2011**, *334*, 965.

[2] M. Capelot, M. M. Unterlass, F. Tournilhac, L. Leibler, *ACS Macro Lett.* **2012**, *1*, 789.

[3] W. Denissen, J. M. Winne, F. E. Du Prez, *Chem. Sci.* **2016**, *7*, 30.

[4] a) M. Capelot, D. Montarnal, F. Tournilhac, L. Leibler, *J. Am. Chem. Soc.* **2012**, *134*, 7664; b) A. Demongeot, S. J. Mougnier, S. Okada, C. Soulié-Ziakovic, F. Tournilhac, *Polym. Chem.* **2016**, *7*, 4486; c) H. Fang, W. Ye, Y. Ding, H. H. Winter, *Macromolecules* **2020**, *53*, 4855; d) F. I. Altuna, U. Casado, I. E. dell'Erba, L. Luna, C. E. Hoppe, R. J. J. Williams, *Polym. Chem.* **2020**, *11*, 1337; e) T. Liu, S. Zhang, C. Hao, C. Verdi, W. Liu, H. Liu, J. Zhang, *Macromol. Rapid Commun.* **2019**, *40*, 1800889; f) F. I. Altuna, C. E. Hoppe, R. J. J. Williams, *Eur. Polym. J.* **2019**, *113*, 297.

[5] a) M. Guerre, C. Taplan, R. Nicolay, J. M. Winne, F. E. Du Prez, *J. Am. Chem. Soc.* **2018**, *140*, 13272; b) W. Denissen, G. Rivero, R. Nicolaÿ, L. Leibler, J. M. Winne, F. E. Du Prez, *Adv. Funct. Mater.* **2015**, *25*, 2451; c) L. Bai, J. Zheng, *Compos. Sci. Technol.* **2020**, *190*, 108062.

[6]   a) P. Haida, V. Abetz, *Macromol. Rapid Commun.* **2020**, *41*, 2000273; b) Z. Q. Lei, P. Xie, M. Z. Rong, M. Q. Zhang, *J. Mater. Chem. A* **2015**, *3*, 19662; c) P. Taynton, K. Yu, R. K. Shoemaker, Y. Jin, H. J. Qi, W. Zhang, *Adv. Mater.* **2014**, *26*, 3938.

[7]   a) J. Han, T. Liu, C. Hao, S. Zhang, B. Guo, J. Zhang, *Macromolecules* **2018**, *51*, 6789; b) J. J. Lessard, L. F. Garcia, C. P. Easterling, M. B. Sims, K. C. Bentz, S. Arencibia, D. A. Savin, B. S. Sumerlin, *Macromolecules* **2019**, *52*, 2105.

[8]   F. Van Lijsebetten, K. De Bruycker, Y. Spiesschaert, J. M. Winne, F. E. Du Prez, *Angew. Chem. Int. Ed.* **2022**, *61*, 202113872.

[9]   a) L. Yue, H. Guo, A. Kennedy, A. Patel, X. Gong, T. Ju, T. Gray, I. Manas-Zloczower, *ACS Macro Lett.* **2020**, *9*, 836; b) Y. Wang, Z. Liu, C. Zhou, Y. Yuan, L. Jiang, B. Wu, J. Lei, *J. Mater. Chem. A* **2019**, *7*, 3577.

[10] C. A. Angell, Y. Ansari, Z. Zhao, *Faraday Discuss.* **2012**, *154*, 9.

[11] K. Ueno, K. Yoshida, M. Tsuchiya, N. Tachikawa, K. Dokko, M. Watanabe, *J. Phys. Chem. B* **2012**, *116*, 11323.

[12] N. Hameed, D. J. Eyckens, B. M. Long, N. V. Salim, J. C. Capricho, L. Servinis, M. De Souza, M. D. Perus, R. J. Varley, L. C. Henderson, *ACS Appl. Polym. Mater.* **2020**, *2*, 2651.

[13] D. J. Eyckens, M. E. Champion, B. L. Fox, P. Yoganantharajah, Y. Gibert, T. Welton, L. C. Henderson, *Eur. J. Org. Chem.* **2016**, *2016*, 913.

[14] D. J. Eyckens, L. C. Henderson, *Front. Chem.* **2019**, *7*, 263.

[15] Z. Zhang, C. P. Wong, *J. Appl. Polym. Sci.* **2002**, *86*, 1572.

[16] D. Brouillette, D. E. Irish, N. J. Taylor, G. Perron, M. Odziemkowski, J. E. Desnoyers, *Phys. Chem. Chem. Phys.* **2002**, *4*, 6063.

[17] W. Zhao, Z. Pan, Y. Zhang, Y. Liu, H. Dou, Y. Shi, Z. Zuo, B. Zhang, J. Chen, X. Zhao, X. Yang, *Angew. Chem. Int. Ed. Engl.* **2022**, *61*, 202205187.

[18] Y. Spiesschaert, M. Guerre, I. De Baere, W. Van Paepegem, J. M. Winne, F. E. Du Prez, *Macromolecules* **2020**, *53*, 2485.

[19] a) C. Tong, in *Advanced Materials for Printed Flexible Electronics*, (Ed: C. Tong), Springer International Publishing, NY **2022**, pp. 221; b) Y. Su, X. Ping, K. J. Yu, J. W. Lee, J. A. Fan, B. Wang, M. Li, R. Li, D. V. Harburg, Y. Huang, C. Yu, S. Mao, J. Shim, Q. Yang, P.-Y. Lee, A. Armonas, K.-J. Choi, Y. Yang, U. Paik, T. Chang, T. J. Dawidczyk, Y. Huang, S. Wang, J. A. Rogers, *Adv. Mater.* **2017**, *29*, 1604989; c) D. C. Kim, H. J. Shim, W. Lee, J. H. Koo, D.-H. Kim, *Adv. Mater.* **2020**, *32*, 1902743.

[20] D. Qi, K. Zhang, G. Tian, B. Jiang, Y. Huang, *Adv. Mater.* **2021**, *33*, 2003155.

[21] M. V. Hoang, H.-J. Chung, A. L. Elias, *J. Micromech. Microeng.* **2016**, *26*, 105019.

[22] a) L. Francioso, C. De Pascali, R. Bartali, E. Morganti, L. Lorenzelli, P. Siciliano, N. Laidani, *ACS Appl. Mater. Interfaces* **2013**, *5*, 6586; b) Y. Kim, K.-H. Nam, Y. C. Jung, H. Han, *Composites, Part B* **2020**, *203*, 108451.

[23] a) W. A. Henderson, N. R. Brooks, W. W. Brennessel, V. G. Young, *Chem. Mater.* **2003**, *15*, 4679; b) W. A. Henderson, N. R. Brooks, V. G. Young, *Chem. Mater.* **2003**, *15*, 4685.

[24] a) S. Tsuzuki, W. Shinoda, S. Seki, Y. Umebayashi, K. Yoshida, K. Dokko, M. Watanabe, *ChemPhysChem* **2013**, *14*, 1993; b) T. Mandai, K. Yoshida, K. Ueno, K. Dokko, M. Watanabe, *Phys. Chem. Chem. Phys.* **2014**, *16*, 8761; c) G. A. Lawrance, *Chem. Rev.* **1986**, *86*, 17.

[25] T. Watkins, D. A. Buttry, *J. Phys. Chem. B* **2015**, *119*, 7003.

[26] S. Di Pietro, V. Bordoni, A. Mezzetta, C. Chiappe, G. Signore, L. Guazzelli, V. Di Bussolo, *Molecules* **2019**, *24*, 2946.

[27] a) J. H. Han, S.-J. Hong, E. Y. Lee, J. H. Lee, H. J. Kim, H. Kwak, C. Kim, *Bull. Korean Chem. Soc.* **2005**, *26*, 1434; b) A. Kamal, R. Ramu, M. A. Azhar, G. B. R. Khanna, *Tetrahedron Lett.* **2005**, *46*, 2675; c) M. Maheswara, K. S. V. K. Rao, J. Y. Do, *Tetrahedron Lett.* **2008**, *49*, 1795; d) T. Hansen, P. Vermeeren, A. Haim, M. J. H. van Dorp, J. D. C. Codée, F. M. Bickelhaupt, T. A. Hamlin, *Eur. J. Org. Chem.* **2020**, *2020*, 3822.

[28] M. Schmeisser, P. Illner, R. Puchta, A. Zahl, R. van Eldik, *Chem. Euro. J.* **2012**, *18*, 10969.

[29] U. Mayer, V. Gutmann, W. Gerger, *Chem. Mon.* **1975**, *106*, 1235.

[30] A. Omrani, M. Ghaemy, A. A. Rostami, *J. Therm. Anal. Calorim.* **2009**, *98*, 477.

[31] W. Denissen, M. Droesbeke, R. Nicolay, L. Leibler, J. M. Winne, F. E. Du Prez, *Nat. Commun.* **2017**, *8*, 14857.

[32] L. Li, X. Chen, K. Jin, J. M. Torkelson, *Macromolecules* **2018**, *51*, 5537.

[33] W. Liu, D. F. Schmidt, E. Reynaud, *Ind. Eng. Chem. Res.* **2017**, *56*, 2667.

[34] H. Ardebili, J. Zhang, M. G. Pecht, in *Encapsulation Technologies for Electronic Applications (Second Edition)*, (Eds: H. Ardebili, J. Zhang, M. G. Pecht), William Andrew Publishing, Norwich, NY **2019**, p. 47.